Pertanika J. Trop. Agric. Sci. 49 (3): 1413 - 1435 (2026)

PERTANIKA JOURNALS

TROPICAL AGRICULTURAL SCIENCE

Journal homepage: http://www.pertanika.upm.edu.my/

Effects of Soil Texture and Moisture on the Performance of EC-based Nutrient Sensor in Humid Tropical Mineral Soils

Melissa Mei Teng Lok[1], Ngai Paing Tan[1], Yei Kheng Tee[2], and Christopher Boon Sung Teh[1]*

[1]Department of Land Management, Faculty of Agriculture, Universiti Putra Malaysia, 43400 Serdang, Selangor, Malaysia

[2]Cocoa Upstream Technology Department, Malaysian Cocoa Board, Sg. Dulang Road, P.O. Box 30, 36307 Sungai Sumun, Perak, Malaysia

ABSTRACT

An electrical conductivity (EC)-based nutrient sensor was tested on 37 Malaysian mineral soils, covering the texture and moisture range of humid tropical conditions, to estimate the apparent electrical conductivity (ECa), NO_3^-, P, and K in real time. The sensor converts the nutrient ionic strength in the soil solution into electrical signals to estimate concentration. Against the 1:5 soil extract EC standard method, it estimated NO_3^- and K well but not P (Kling-Gupta Efficiency, KGE = 0.31), since orthophosphate ions contribute little to overall ionic strength. Soils were subjected to 13 moisture treatments ranging from 0% to 60% (w/w) to assess the EC-based nutrient sensor's performance. The study found that the sensor performed well (achieving KGE > 0.50, a mean absolute error <50%, and a bias error between -6% and 7%) in soils with clay content below 40% (v/v) and moisture levels above the saturation point (flooding conditions). However, results also indicated that the sensor underperformed in drier soils or clay content above 40% (achieving KGE<0.39, a mean absolute error >48%, and a bias error between -26% and 11%) due to insufficient soil water for nutrient dissolution and reduced ionic mobility. These limitations must be considered when integrating EC-based nutrient sensors into IoT-based field data acquisition systems for real-time soil nutrient monitoring**.** While technological limitations remain, overcoming these challenges will allow this in-situ sensing framework to effectively characterise soil nutrient dynamics and establish the environmental thresholds necessary for precision, 'right-time' fertiliser management.

Keywords: Electrical conductivity, nitrate, potassium, precision agriculture, soil nutrient estimation

ARTICLE INFO

Article history:
Received: 12 August 2025
Accepted: 09 June 2026
Published: 26 June 2026

DOI: https://doi.org/10.47836/pjtas.49.3.21

E-mail addresses:
melissa.meiteng@gmail.com (Melissa Mei Teng)
ngaipaing@upm.edu.my (Ngai Paing Tan)
tee_yei@koko.gov.my (Yei Kheng Tee)
chris@upm.edu.my (Christopher Boon Sung Teh)
* Corresponding author

e-ISSN: 2231-8542

INTRODUCTION

Nutrient content, particularly nitrogen (N), phosphorus (P), and potassium (K) - collectively known here in this paper as NPK - is important in supporting plant health and crop production (Žinete, 2023). To understand the soil nutrient status, soil nutrient analysis plays a pivotal role in sustainable agricultural development by ensuring balanced fertilisation, improving crop performance, and mitigating environmental degradation (Sahu et al., 2020). Traditional laboratory-based soil testing methods are the benchmark for accuracy, but they are time-consuming, expensive, and require specialised equipment and trained personnel. These limitations make them less practical for on-site or real-time decision-making, especially for resource-limited farmers.

Hence, innovative solutions are essential for delivering real-time, precise data on soil nutrient levels and addressing the limitations of traditional laboratory nutrient analysis (Islam et al., 2023). In recent years, the application of Internet of Things (IoT) technology for real-time soil nutrient monitoring has emerged (Reddy et al., 2023). The integration of EC-based nutrient sensors with IoT has enhanced resource efficiency by enabling real-time monitoring, reducing operational costs, and facilitating data-driven decisions through artificial intelligence in fertilisation systems. This has led to more sustainable and productive agriculture (Hossain et al., 2023; Nyakuri et al., 2022).

The EC-based nutrient sensor operates on the principle of apparent electrical conductivity (ECa), measuring bulk soil conductivity in real-time to estimate nutrient content.(Corwin & Yemoto, 2020). Nevertheless, ECa is influenced by soil texture. Clay soils hold more water gravimetrically than sandy soils; therefore, the former soils have greater water-holding capacity (Rout & Arulmozhiselvan, 2019). That difference affects ECa, and measurements lose reliability under fluctuating moisture (Costa et al., 2014), complicating nutrient estimation in heterogeneous soils.

The ECa-nutrient relationship is inconsistent across soil types, spatial gradients, and cropping systems, with location-specific factors adding further noise (Heiniger et al., 2003; Mazur et al., 2022; Omonode & Vyn, 2006). Fertiliser applications temporarily raise EC, but the increase does not consistently correspond to nutrient availability across soils (Othaman et al., 2021). EC-based sensors have advanced, allowing for real-time nutrient monitoring, but the diverse physical and chemical properties of soils prevent them from fully capturing soil-nutrient interactions, producing errors under variable field conditions.

Although Dimkpa et al. (2017) found few independent assessments of rapid nutrient testing technologies, sensor accuracy remains under-documented in the literature. Most studies have integrated EC sensors into IoT frameworks for real-time monitoring without validating accuracy across soil textures and moisture levels. Soil texture, moisture content, chemical composition, and microbial communities each shift readings independently, making direct nutrient detection unreliable (Nadporozhskaya et al., 2022). This limits

EC-based sensors in heterogeneous tropical agricultural soils, which are predominantly weathered and acidic and cover about 43% of Earth's land area (Nottingham et al., 2022). These sensors warrant further investigation, though their reliability remains constrained by soil heterogeneity and dynamic field conditions.

This study evaluated an EC-based nutrient sensor across varied soil textures and moisture conditions in selected tropical mineral soils. The sensor design is specific, but the findings address the broader relationships among soil EC, moisture, and NO_3^-, P, and K captured by EC-based devices. Performance was assessed through simple linear regression models validated against laboratory data using three metrics: Kling-Gupta Efficiency (KGE), Normalised Mean Absolute Error (NMAE), and Normalised Mean Bias Error (NMBE). Understanding how the sensor performs across soil conditions will inform strategies for reliable soil fertility monitoring.

This study focuses on selected Peninsular Malaysian mineral soils, which are taken as representative of humid tropical soils. These soils are characterised by intense weathering, significant nutrient leaching, acidity ($pH < 5$), low cation exchange capacity ($CEC < 20$ cmol/kg), low total phosphorus ($\leq 24\%$), high exchangeable aluminium in some areas, and a predominance of Oxisols with a silt-to-clay ratio of less than 0.15. Oxisols cover approximately 23% of the Earth's land area (Dion, 2010; Nottingham et al., 2022) .

Unlike previous studies that primarily focus on IoT frameworks, this study uniquely investigates the responses of an EC-based nutrient sensor in determining nutrients (EC, NPK) under varying soil moisture and texture conditions in Malaysian mineral soils, which are representative of humid tropical environments. However, due to the specificity of humid tropical soil properties, the findings should be interpreted with caution when applied to other soil types beyond this region.

EC-based sensors offer a faster alternative to laboratory testing for real-time soil fertility monitoring, but how soil texture and moisture affect bulk conductivity and NPK estimation in humid tropical mineral soils is still not well characterised. Consequently, this study aimed to evaluate how both variables influence EC-based sensor performance for estimating these macronutrients, hypothesising that texture and moisture alter ECa by governing water availability and ion mobility, which affects estimation accuracy.

MATERIALS AND METHODS

Soil Sampling and Laboratory Soil Assays

To capture a wide range of soil physical and chemical properties—particularly soil texture variations—at selected field sites in Malaysia representing tropical mineral soils, a point sampling approach was employed. Individual soil samples were collected from distinct locations, each representing different soil types, land uses, and agroecological conditions (Figure 1). This approach captured diverse soil characteristics rather than spatial variability

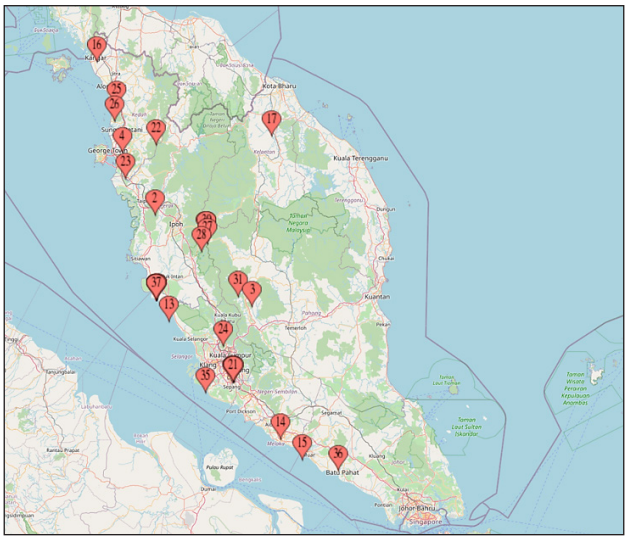

Figure 1. Spatial distribution of the 37 soil sampling locations across Peninsular Malaysia, representing diverse soil textures, land uses, and agroecological zones

within a single field. Sampling was carried out in 2024 across locations with a humid tropical climate, high temperatures, and variable rainfall. Thirty-seven topsoil samples (0-10 cm) were selected using a point sampling approach, spanning a regional gradient of soil textures, parent materials, and crop management histories. This layer is the primary zone of root activity and fertiliser application. Samples were air-dried, ground, and sieved through a 2-mm mesh. Air-dried soil forms hard clumps that can damage the probe, so crushing and sieving were necessary before sensor insertion. Laboratory assays characterised soil chemical and physical properties (Table 1 and Table 2). All laboratory characterisation and sensor measurements were conducted in triplicate.

For soil chemical properties, the following parameters were measured: pH, EC, total nitrogen (TN), NH_4^+, NO_3^-, available P, and exchangeable K. These analyses followed the protocols outlined by Reeuwijk (2002), Gavlak et al. (2005), and Pansu et al. (2006).

The pH and EC of the suspension were measured using a Hanna Edge pH meter and a Hanna HI2300 EC meter (Hanna Instruments, USA). NH_4^+ and NO_3^- concentrations in the filtrate were analysed using a SEAL AA500 AutoAnalyzer (SEAL Analytical, Germany). Available P was measured using a Series 1000 UV/Visible Spectrophotometer (Cecil Instruments, UK) at 882 nm. Exchangeable K was determined using a PinAAcle 900T Atomic Absorption Spectrometer (PerkinElmer, USA).

Soil physical properties, including soil texture, were determined according to the methods described by Gee & Bauder (1986), and soil water retention was measured using the procedure outlined by Klute (1986).

Table 1
Chemical properties and dataset categorisation of soil samples

Sample	TN	NH_4^+	NO_3^-	Available P	Exchangeable K	pH	EC	Dataset Purpose
	%	mg kg^{-1}					µS cm^{-1}	
1	0.13	20.2	1.4	92.9	1468.4	6.2	156.5	Calibration
2	0.12	36.2	8.1	10.6	400.8	3.9	72.4	
3	0.14	29.9	2.0	15.4	452.3	5.8	55.1	
4	0.15	29.9	24.5	10.9	540.6	4.5	91.0	
5	0.14	30.8	22.7	144.1	1495.3	5.4	64.4	
6	0.10	32.7	8.6	247.4	448.8	4.8	49.2	
7	0.05	29.2	12.7	466.8	465.8	5.1	62.9	
8	0.10	22.4	4.9	54.4	647.1	4.7	56.8	
9	0.18	28.9	2.0	54.4	740.0	5.8	23.9	
10	0.19	38.2	8.8	133.5	946.0	5.1	31.1	
11	0.22	37.9	30.0	3057.0	3192.4	7.0	200.9	
12	0.04	0.2	N/A	9.6	691.2	5.9	17.5	
13	0.10	25.9	93.4	220.6	5311.0	6.4	460.3	
14	0.13	36.1	66.0	1466.2	3528.7	7.2	188.8	
15	0.15	28.2	22.7	28.7	464.4	4.8	20.8	
16	0.20	30.3	1.1	136.9	1532.1	4.7	44.6	
17	0.15	25.1	5.9	255.1	1716.1	6.6	146.0	
18	0.19	24.3	6.6	221.7	2483.6	7.1	93.4	
19	0.19	32.7	7.6	354.5	5340.1	7.4	147.2	
20	0.40	18.9	6.4	363.1	1179.4	4.5	283.9	
21	0.12	42.1	18.8	94.0	438.1	4.7	62.2	
22	0.08	20.4	0.6	105.1	491.6	6.8	78.1	
23	0.18	20.4	8.3	261.0	1617.4	7.2	91.3	
24	0.09	22.8	0.3	18.9	869.6	4.4	44.3	

Table 1 (*continued*)

Sample	TN	NH_4^+	NO_3^-	Available P	Exchangeable K	pH	EC	Dataset Purpose
	%	mg kg^{-1}					µS cm^{-1}	
25	0.06	23.5	N/A	29.9	999.0	6.0	58.3	
26	0.08	20.0	20.9	48.8	775.9	5.8	106.5	
27	0.12	34.1	10.8	21.2	709.3	5.8	84.1	Validation
28	0.20	40.0	22.6	77.6	487.6	4.5	50.7	
29	0.24	34.3	8.5	45.7	799.0	5.0	53.9	
30	0.14	23.6	16.0	28.9	456.5	5.7	77.5	
31	0.14	28.9	70.0	561.4	5897.0	6.9	401.0	
32	0.18	28.0	6.6	228.3	1773.0	6.2	103.1	
33	0.21	24.4	18.3	400.9	3335.1	6.7	245.9	
34	0.08	19.6	8.2	234.4	513.6	7.2	87.7	
35	0.12	31.3	34.7	20.2	1248.6	4.7	130.0	
36	0.05	18.9	0.5	47.5	388.6	6.6	75.6	
37	0.09	21.9	24.6	171.2	1486.7	6.4	155.2	

Note. N/A: Not available

Table 2
Physical properties, sampling locations, and land use of soil samples

Sample	SP	FC	PWP	USDA Texture (%clay, %sand)	Location °N, °E	Land Use
	%					
1	44	29	22	C (59, 13)	3.656278, 101.008444	Cocoa (*Theobroma cacao*)
2	37	20	14	SCL (34, 54)	3.001083, 101.724556	Pine (*Pinus spp.*)
3	38	22	18	C (59, 35)	2.988389, 101.724500	Oil palm (*Elaeis guineensis*)
4	39	22	17	C (57, 38)	2.987972, 101.728000	Oil palm
5	34	21	15	CL (39, 30)	5.602833, 100.861028	Vegetables
6	26	6	4	LS (8, 87)	5.233528, 100.527111	Vegetables
7	25	8	4	LS (6, 88)	3.381000, 101.608500	Vegetables
8	34	20	14	SCL (34, 46)	2.355306, 102.245722	Cocoa
9	41	27	20	C (52, 11)	6.026056, 100.421083	Paddy (*Oryza sativa*)
10	38	22	11	SL (17, 56)	5.870167, 100.403528	Paddy
11	41	21	14	SL (14, 61)	4.511222, 101.433611	Vegetables
12	41	27	21	C (44, 43)	4.425639, 101.368278	Open land (Cleared Forest)
13	40	25	19	C (42, 35)	4.589389, 101.419972	Vegetables
14	39	23	15	SL (19, 56)	4.590750, 101.422778	Vegetables
15	35	22	14	L (24, 40)	3.931667, 101.774472	Durian (*Durio zibethinus*)
16	46	34	27	C (66, 2)	3.895806, 100.868222	Cocoa
17	45	32	24	SiC (51, 8)	3.897778, 100.869500	Cocoa
18	47	33	26	C (67, 1)	3.900222, 100.872222	Cocoa
19	45	32	24	C (62, 5)	3.899167, 100.869722	Cocoa
20	47	28	18	CL (28, 40)	2.867944, 101.414694	Oil palm

Table 2 (*continued*)

Sample	SP	FC	PWP	USDA Texture (%clay, %sand)	Location °N, °E	Land Use
	%					
21	35	20	10	SL (16, 63)	2.000111, 102.889444	Water discharge from an Arowana (*Scleropages formosus*) fishpond area
22	28	8	4	LS (6, 88)	3.895778, 100.869167	Cocoa
23	40	27	19	C (48, 20)	3.895806, 100.868222	Cocoa
24	40	27	19	C (56, 10)	2.123222, 102.492694	Cocoa
25	30	15	7	L (18, 52)	6.528056, 100.203528	Cocoa
26	35	17	6	SL (14, 72)	5.707917, 102.149333	Cocoa
27	37	18	13	SC (40, 51)	2.982611, 101.709556	Coconut (Cocos nucifera)
28	37	18	12	SCL (31, 61)	2.982722, 101.724056	Rubber (*Hevea brasiliensis*)
29	43	28	23	S (68, 23)	2.982472, 101.722417	Coconut
30	32	11	7	SL (16, 78)	2.988750, 101.723194	Oil palm
31	39	25	18	CL (30, 43)	4.590222, 101.421917	Vegetables
32	44	32	25	SiC (58, 1)	3.896556, 100.864778	Cocoa
33	44	32	24	C (65, 1)	3.910000, 100.871417	Cocoa
34	28	10	5	LS (9, 86)	3.893778, 100.864861	Cocoa
35	38	21	16	SC (48, 47)	4.824278, 100.857556	Cocoa
36	29	12	5	SL (16, 65)	3.820083, 101.932194	Cocoa
37	34	20	12	CL (29, 43)	5.519472, 100.495333	Cocoa

Note. SP: Saturated point (wet basis). FC: Field capacity (wet basis). PWP: Permanent wilting point (wet basis). C: Clay. CL: Clay loam. L: Loam. LS: loamy sand. SCL: Sandy clay loam. SL: sandy loam. SC: Sandy clay. SiC: Silty clay

Relationship between EC and NPK in Laboratory Analysis

The soil EC and NPK data were obtained through laboratory analysis and further investigated to determine their relationship. A total of 37 soil samples were used in this study. Pearson correlation analysis was first conducted to assess the strength and direction of the relationships between EC and the concentrations of TN, NH_4^+, NO_3^-, P, and K across all 37 soil samples. A minimum correlation threshold of $r \geq 0.60$ was set as a prerequisite for subsequent regression development. Setting this threshold at this level will determine EC's predictive power for these nutrients.

The 37 soil samples were randomly divided into calibration and validation groups in a 70:30 ratio, respectively, where the calibration group, comprising 26 soil samples, was utilised to construct simple linear regression models to predict nutrient concentrations based on laboratory EC values. 95% confidence intervals were calculated for all regression coefficients to establish parameter precision. The validation group, comprising 11 samples, was for independent validation. These allocations are detailed in Table 1 under the 'Dataset Category', with 26 samples designated for calibration and 11 for validation using R statistical software (version 4.3.1).

Validation of the models' prediction performance was assessed using three statistical metrics: KGE, NMAE, and NMBE. The last two metrics were selected to assess overall model accuracy and model bias, respectively, whereas KGE was chosen because it simultaneously assesses a model's performance based on three criteria: correlation, bias, and variability between observed and predicted values. KGE ranges from $-\infty$ to 1, with a value of 1 indicating perfect agreement. NMAE measures the average prediction error normalised to the observed range, allowing for an evaluation of how closely the predictions align with observed values, where values range from 0 to $+\infty$, with 0 indicating perfect agreement. NMBE quantifies model bias, offering insight into whether the predictions systematically overestimate or underestimate observations, with values ranging from $-\infty$ to $+\infty$ and 0 indicating no bias (Gupta et al., 2009)

$$KGE = 1 - \sqrt{(r-1)^2 + (\beta-1)^2 + (\gamma-1)^2} \quad [1]$$

where r is the correlation coefficient between predicted and observed values; β is the bias ratio, defined as μp/μo, where μp is the mean predicted value, and μo is the mean observed value (both expressed in the same unit); and γ=(σ_o⁄μ_0)/(σ_p⁄μ_p) the variability ratio, which compares the observed coefficient of variation (σo/μo) to the predicted coefficient of variation (σp/μp).

$$NMAE = \frac{\sum_{i=1}^{n} |Pi - Oi|}{n \times \bar{O}} \quad [2]$$

where Pi represents the predicted values; represents the observed values; Ō represents the mean of all observed values, respectively (all in the same unit); n represents the total number of observations.

$$NMBE = \frac{\sum_{i=1}^{n}(Pi-Oi)}{n\times\bar{O}} \quad [3]$$

These three metrics (Equations 1 - 3) were chosen for their distinct strengths: KGE combines correlation, bias, and variability into a single score for overall model fit; NMAE measures overall model prediction errors; and NMBE measures model bias, revealing whether the model consistently over- or under-predicts.

Together, these metrics assess both the EC-nutrient relationship and the practical reliability of the regression models for estimating nutrient concentrations from EC measurements.

Evaluation of an EC-based Electronic Nutrient Sensor under Various Soil Moisture Conditions

The EC-based electronic nutrient sensor, manufactured by JXCT® (Shandong Jingxunchangtong Electronic Technology Co., Ltd., China), has two stainless steel electrodes that measure soil NPK, temperature, moisture, pH, and EC (Figure 2). The probes are IP68-rated, use an RS485 output signal, and operate at 9-24 V DC. Data are displayed on the sensor monitor.

Soil moisture was controlled in a laboratory to isolate its effect on sensor performance from field variables such as evaporation under direct sunlight.

Moisture levels were adjusted from 0% to 60% (w/w) at 5% intervals. The 60% ceiling was set to exceed the saturation point (wet basis) of each soil, enabling evaluation under

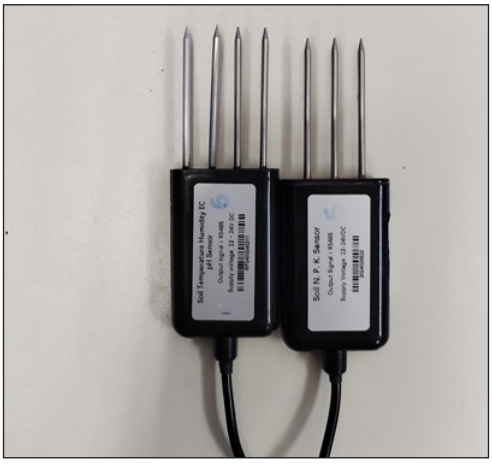

Figure 2. Stainless steel soil NPK, temperature, moisture, EC and pH electrical probes

fully saturated conditions. For a 250 g subsample, 12.5 g of water (5% of 250 g) was added per step. After each addition, subsamples were equilibrated for one day to allow uniform water distribution before sensor measurements.

At each moisture level, sensor readings were taken after 1 min for all three subsamples of each soil (Figure 3). Soil moisture (v/v) was measured immediately after using a FieldScout TDR 100 (Spectrum Technologies, Inc., USA). This sensor was calibrated before each use and served as a moisture reference, given its established use in soil moisture determination. These readings were compared against the saturation point (SP, wet basis) measured for each soil using the pressure plate extractor method. Full saturation was confirmed when TDR readings stabilised at each soil's SP threshold.

Optimisation and Evaluation of EC-Based Electronic Nutrient Sensor

A total of 1,443 sensor readings were collected by monitoring the 37 soil samples across sequential moisture content adjustments, ranging from 0% to 60% (w/w) at 5% intervals. To evaluate sensor performance against laboratory values across varying moisture matrices,

Figure 3. Soil parameters determination using EC-based electronic nutrient sensor (Shandong Jingxunchangtong Electronic Technology Co., Ltd., China)

the dataset was partitioned strictly by soil sample, matching the independent 26-calibration and 11-validation sample groupings detailed in Table 1, was applied to categorise the data into calibration and validation sets.

To optimise the performance of the electronic in-situ nutrient sensor, data were filtered based on soil moisture conditions measured using the FieldScout TDR 100 soil moisture meter and soil texture. Specifically, soil texture was filtered by clay percentage to ensure the calibration models accurately accounted for the physical properties influencing nutrient estimation. A simple linear regression modelling approach was employed to develop predictive models linking the electronic in-situ sensor values (EC, NO_3^-, P, and K) to laboratory-determined soil nutrient concentrations. Sensor performance was evaluated using three statistical metrics—KGE, NMAE, and NMBE—to ensure accuracy and reliability across diverse soil conditions.

RESULTS AND DISCUSSIONS

Relationship between EC and NPK in Laboratory Analysis

EC and forms of N

TN is commonly analysed in the laboratory to understand the combined amount of organic and inorganic N in the soil. While NH_4^+ and NO_3^- represent the inorganic forms of N that are directly available for plant uptake and are the primary sources derived from nitrogen fertilisers.

From Figure 4 **(**a) and (b), no significant relationships were observed between EC and TN or NH_4^+ from laboratory analysis. This lack of correlation can be attributed to NH_4^+ , which is positively charged and strongly adsorbs onto negatively charged soil particles, such as clay minerals. This adsorption reduces its mobility in the soil (Yu et al., 2023). Moreover, soil TN comprises organic forms like proteinaceous materials and heterocyclic compounds, as well as inorganic forms such as ammonia. Many of these N sources are not part of the soil solution, thus not contributing directly to ionic conductivity (Schulten & Schnitzer, 1997). As a result, laboratory EC measurements were less effective in predicting TN or NH_4^+ concentrations due to lower ionic conductivity strength.

In contrast, Figure 4 **(**c) shows a strong positive correlation between EC and NO_3^- concentrations ($r = 0.75$), indicating that higher EC levels correspond to increased NO_3^- content in the soil. This relationship is attributed to NO_3^- is high mobility in water and a significant contribution to soil ionic conductivity. Analysis of 26 soil samples with varying land uses and chemical and physical properties revealed that NO_3^- concentrations can be estimated as 16% of EC values (Figure 4 (d)).

According to Thiemig et al. (2013), KGE values can be classified into performance levels: poor performance ($0.50 > KGE > 0$), intermediate performance ($0.75 > KGE > 0.50$), and good performance ($KGE > 0.75$). Based on this classification, the NO_3^- model

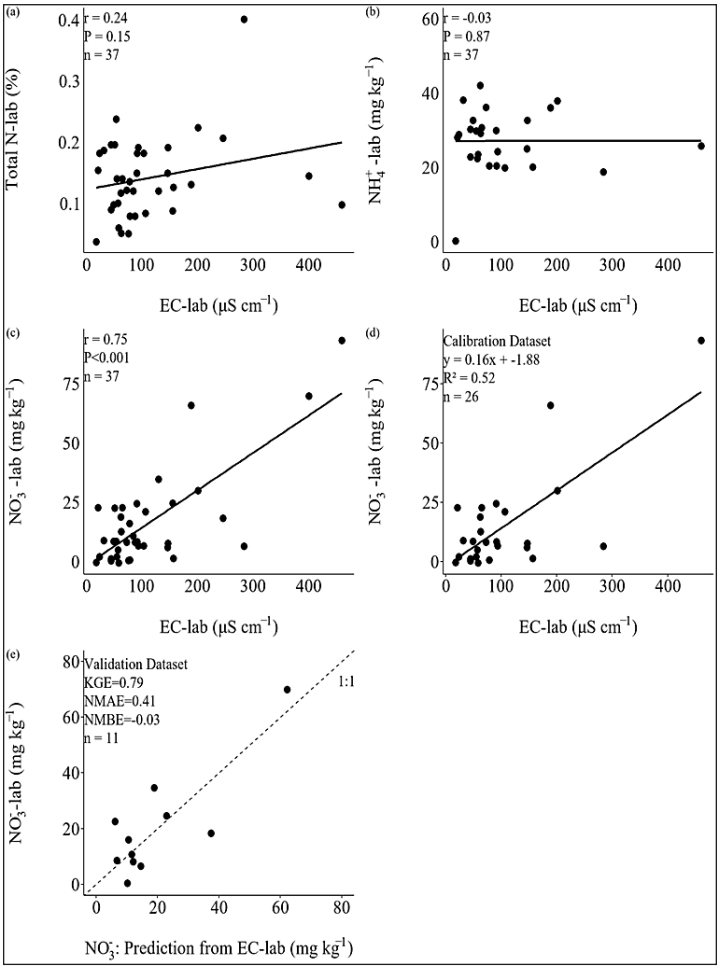

Figure 4. Relationships between laboratory-measured EC and total nitrogen (TN) concentrations (a), EC and NH_4^+ concentrations (b), and EC and NO_3^- concentrations (c); (d) NO_3^- prediction model; and (e) NO_3^- prediction using 1:5 EC values

demonstrates good performance (KGE = 0.79) (Figure 4 (e)), indicating its reliability for predicting nitrate concentrations by EC with moderate error (NMAE = 0.41) and minimal bias (NMBE = -0.03). These findings are consistent with previous studies, highlighting the potential of EC-based regression models, such as those using TDR sensors and the Rhoades model, for continuous monitoring of soil nitrate levels in Andisol fields (Miyamoto et al., 2015).

EC and P

A moderate positive correlation (r = 0.60) was observed between EC and P in laboratory analysis after excluding two outlier samples with extremely high phosphorus concentrations

(>1000 mg kg^{-1}) from the 37 soil samples (Figure 5 (a)). These outliers were identified and removed based on the interquartile range (IQR) method, as the extreme values were attributed to localised over-fertilisation of phosphorus. However, Figure 5 (c) indicate that the P prediction model based on EC had poor performance (KGE=0.31) and 63% mean absolute error. Orthophosphate ions (plant-available P) have lower ionic conductivity in soil solution than nitrate and high natural variability. P availability is governed by pH, mineralogy, microbial solubilization, and organic matter interactions. Iron oxyhydroxides, struvite, vivianite, and organic matter adsorb and precipitate P, while certain bacteria enhance availability by producing organic acids that solubilise bound P, particularly in acidic soils (Ahmed et al., 2023; Azam et al., 2019; Herndon et al., 2020; Tamad et al., 2020). This variability across soils makes P concentration difficult to estimate from EC measurements alone.

EC and K

K correlated positively with EC (r = 0.64, Figure 6a) across selected Malaysian agricultural soils. This is expected because cations, including potassium, calcium, and magnesium, drive soil electrical conductivity, and their concentration and mobility in the soil solution determine EC readings (Rhoades et al., 1989).

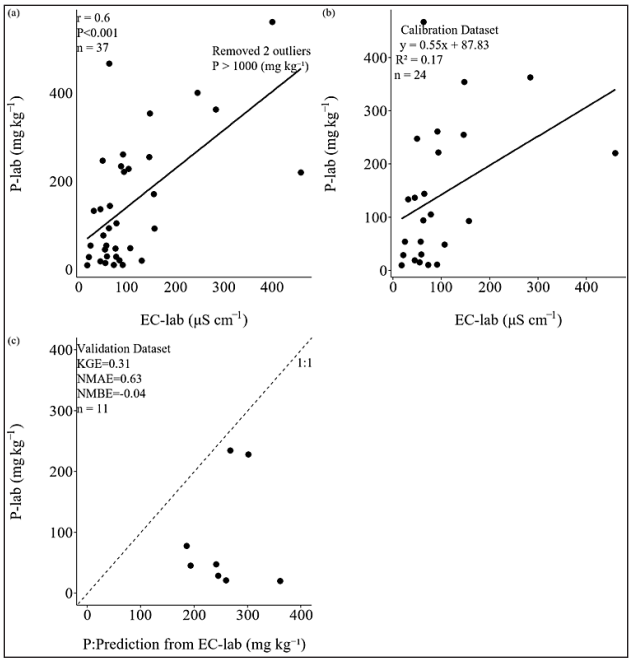

Figure 5. (a) Relationships between laboratory-measured EC and P concentrations; (b) P prediction model; and (c) P prediction using 1:5 EC values

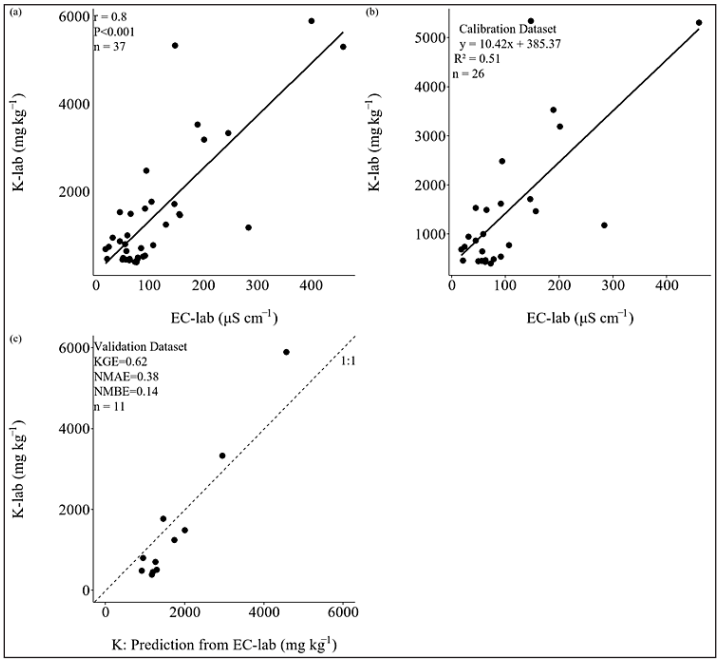

Figure 6. (a) Relationships between laboratory-measured EC and K concentrations; (b) K prediction model; and (c) K prediction using 1:5 EC values

The K prediction model was overall accurate (KGE = 0.62, Figure 6c), capturing the trends in exchangeable K across the sampled soils. The 1:5 soil-to-water EC extraction method estimated K concentrations with sufficient accuracy for rapid nutrient determination.

Optimisation and Evaluation of an Electronic EC-based Nutrient Sensor

The electronic nutrient sensor relies on ECa to estimate soil NPK concentrations, with soil moisture content significantly affecting sensor readings. Figure 7 showed that readings of the sensor for ECa, NO_3^-, P, and K spiked then stabilised once soil moisture exceeded the saturation point in loamy sand. This moisture dependence makes the sensor unsuitable for dry soil conditions.

Moreover, this study revealed that soil texture also affected the sensor's performance to optimise its functionality. The sensor was suitable for applications where clay content was below 30%, with soil moisture (v/v) ranging from 40% to 55% for NO_3^-. While the sensor was effective with clay content below 40%, and soil moisture (v/v) ranging from 40% to 60% for EC, P, and K determination (Table 3). The sensor's best performance was at 40-60% (v/v) moisture because of greater dissolved nutrients and higher ionic conductivity in the soil solution. Higher moisture facilitates mobile nutrient transport (Bauke et al., 2022), and in low-clay soils, NO_3^-, P, and K become more available, increasing ionic conductivity and improving nutrient estimation. At lower moisture levels, nutrient dissolution and mobility

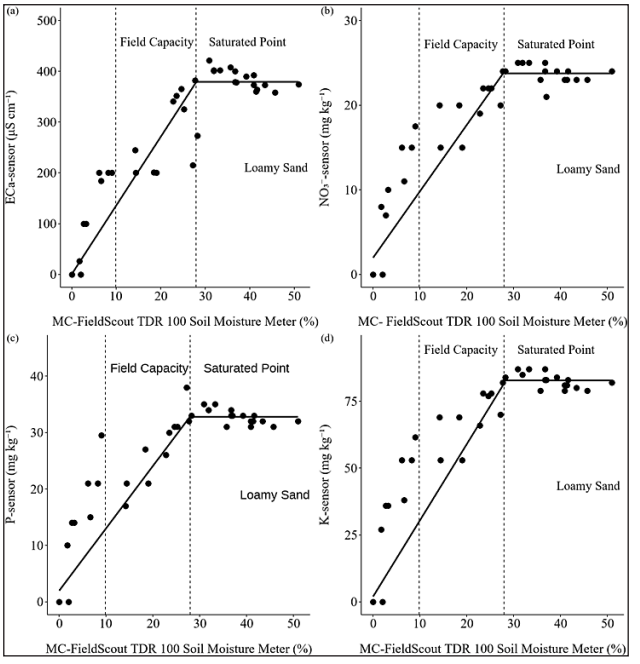

Figure 7. Performance of the EC-based nutrient sensor under varying soil moisture in loamy sand: a) EC response, b) NO3- response, c) P response and d) K: response

Table 3
Criteria for EC-based electronic nutrient sensor

Parameter	MC reading from FieldScout Soil Moisture Meter (%) (v/v)	Clay (%)
EC	40<MC<60	<35
NO_3^-	40<MC<55	<35
P	40<MC<60	<40
K	40<MC<60	<40

Note. MC: soil moisture content. The EC-based electronic nutrient sensor is valid for P concentrations below 1000 mg kg^{-1}

are limited, resulting in less reliable readings. Conversely, excessive moisture beyond the saturation point can also dilute nutrient concentrations, reduce sensor accuracy, and negatively affect the soil environment, such as nutrient leaching.

The EC-based electronic nutrient sensor readings required calibration to achieve accurate results, as outlined in the criteria in Table 3. The calibration models for EC, NO_3^-, P, and K demonstrated intermediate performance, achieving KGE > 0.50, NMAE < 0.50, and $-0.06 \leq NMBE \leq 0.07$ (Figure 8). While these metrics indicate the potential of the models for rapid nutrient estimation, they also highlight room for improvement, especially for high-precision applications.

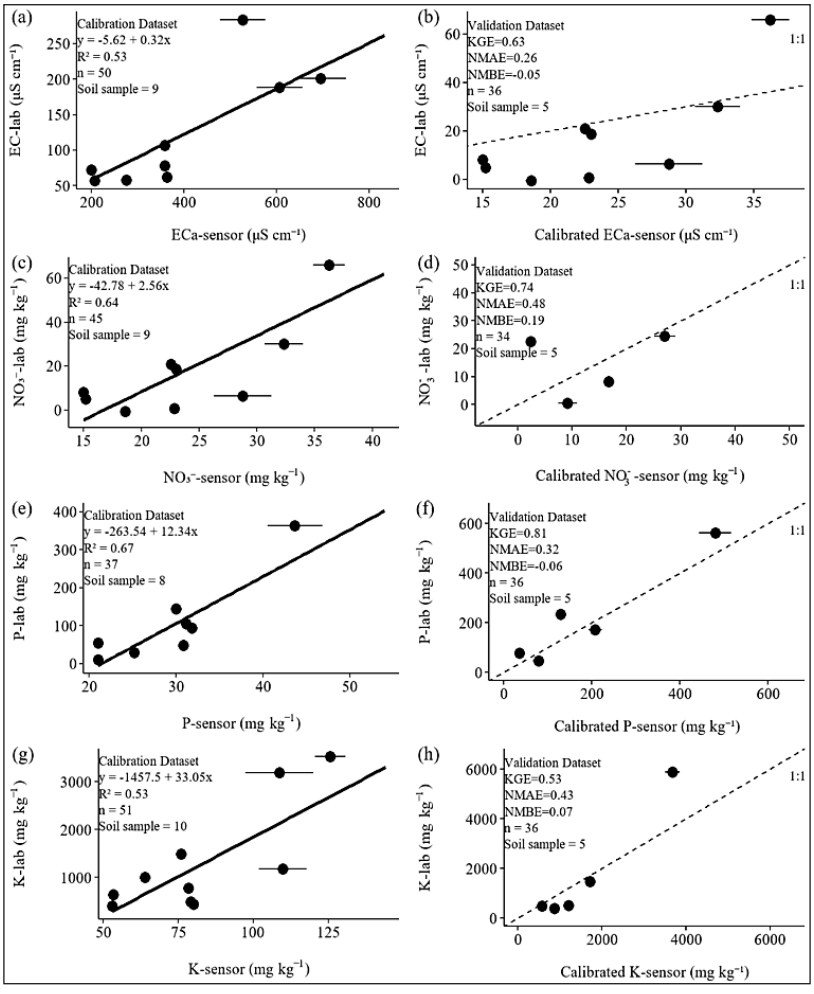

Figure 8. Calibration analysis and validation of the EC-based electronic nutrient sensor against laboratory-measured values, with criteria outlined in Table 3. Error bars represent the mean (± standard error). (a) EC calibration model; (b) EC validation; (c) NO_3^- calibration model; (d) NO_3^- validation; (e) P calibration model; (f) P validation; (g) K calibration model; and (h) K validation

Despite the applicability of these calibration models, the deployment of EC-based electronic nutrient sensors presents two major challenges: soil type specificity and the necessity for high soil moisture levels. When the soil conditions have a clay percentage higher than 30-40% and soil moisture within the range of 10-40% (v/v) (field capacity range) as measured by the FieldScout Soil Moisture Meter, the electronic nutrient sensor performs poorly in estimating soil nutrients (Figures 9 and 10). This is because sandy and silty soils are negatively correlated with CEC, whereas clayey soils have a positive impact on CEC (Obalum et al., 2013), allowing them to retain more nutrients, while CEC is often

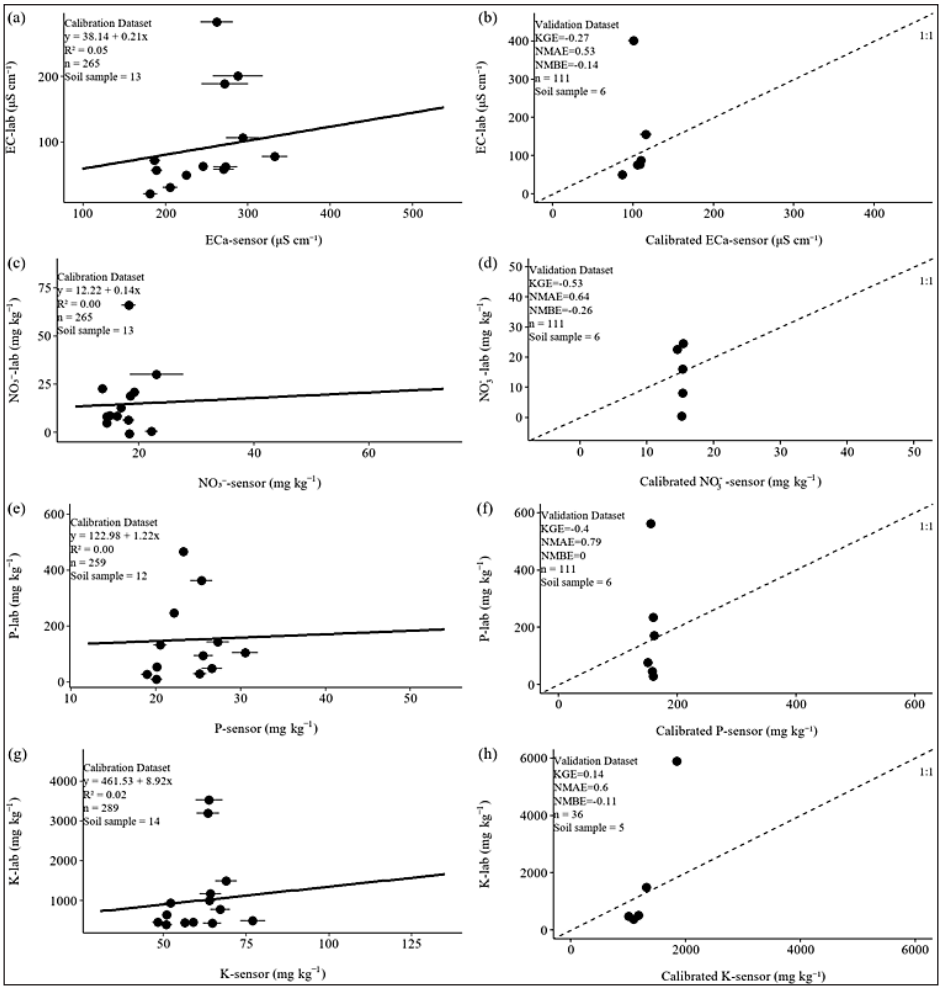

Figure 9. Calibration and validation analysis of the EC-based electronic nutrient sensor against laboratory-measured values, with moisture content within the field capacity range (10-40% v/v) as measured using the FieldScout Soil Moisture Meter. Error bars represent the mean (± standard error). (a) EC calibration model; (b) EC validation; (c) NO_3^- calibration model; (d) NO_3^- validation; (e) P calibration model; (f) P validation; (g) K calibration model; and (h) K validation

correlated with ECa (Zhao et al., 2022). Furthermore, the sensor does not perform optimally at field capacity due to the lower availability of dissolved ions in soil water to convert electrical signals. Soils with clay content above 40% are unsuitable for this sensor. Stable readings also require 40-60% (v/v) moisture, which exceeds the saturation point of most soils. Sustained saturation causes flooding, creating anaerobic conditions that inhibit root function and can trigger root rot (Chadha et al., 2019). Field deployment must therefore account for clay content and moisture management.

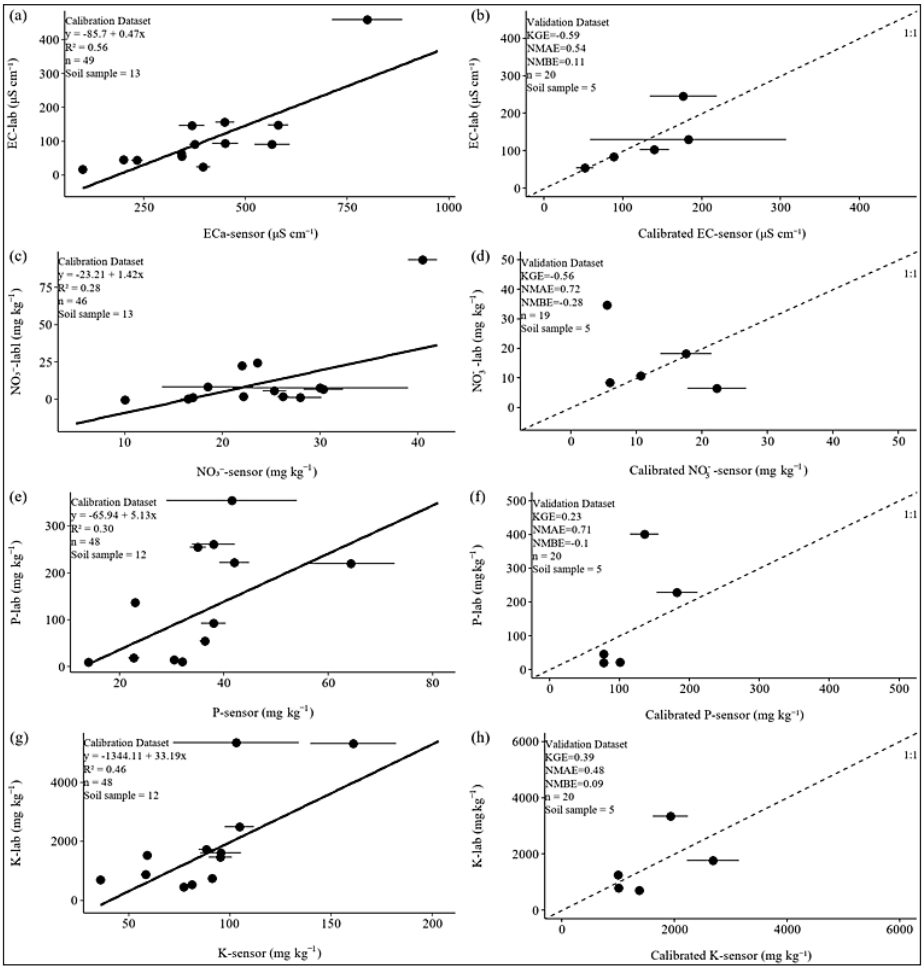

Figure 10. Calibration analysis and validation of the EC-based electronic nutrient sensor against laboratory-measured values, with clay percentage criteria higher than those outlined in Table 3. Error bars represent the mean (± standard error). (a) EC calibration model; (b) EC validation; (c) NO_3^- calibration model; (d) NO_3^- validation; (e) P calibration model; (f) P validation; (g) K calibration model; and (h) K validation

CONCLUSION

This study demonstrates that electronic EC-based sensors provide a viable means of estimating NO_3^- and K levels in humid tropical mineral soils, though their efficacy is strictly influenced by soil physical properties. The 1:5 EC extraction method reliably estimated NO_3^- and K but not P, where the low ionic contribution of orthophosphate produced a poor model fit (KGE = 0.31). The sensor is also restricted to soils below 40% clay; above that threshold, predictive accuracy drops. Performance peaks at near-saturated moisture, though that range risks anaerobic conditions in the root zone. Implementing EC-based sensors in tropical agriculture will require calibration models that account for high clay content and variable moisture regimes.

IMPLICATION OF THE STUDY

Results from this study inform sensor integration for precision agriculture in tropical regions. EC-based sensing works for N and K but not P, which shapes nutrient management protocols accordingly. Texture-specific calibration is necessary: the 40% clay threshold marks where sensor accuracy breaks down. The moisture dependency suggests future designs should incorporate secondary transducers or compensatory logic to remain functional at field capacity. These constraints should guide IoT-based monitoring deployment and ensure data-driven fertilisation accounts for the electrochemical and physical properties of humid tropical mineral soils.

LIMITATION AND RECOMMENDATION FOR FUTURE RESEARCH

The small sample size may limit the generalizability of findings across the full range of humid tropical mineral soils. The results confirm that EC-based sensors face substantial limitations in estimating NO_3^-, P, and K in heterogeneous tropical soils, despite their widespread integration into IoT platforms for real-time monitoring. Future research should draw on a wider range of soils and incorporate geospatial approaches, including fuzzy logic, geostatistical methods, and GIS techniques (Seyedmohammadi et al., 2019), to improve calibration and site-specific nutrient estimation. Sensor design should also target sensitivity and reliability at field capacity, which better represents actual growing conditions. In regions with high soil variability, precision agriculture adoption should proceed cautiously, with priority given to localised calibration.

ACKNOWLEDGEMENT

The authors express their gratitude to the Malaysian Cocoa Board for the financial support provided for this research under grant P20001001210010, titled “Pertanian Pintar ke Arah Pengurusan Koko Secara Digital (RMK-12).”

DATA AVAILABILITY STATEMENT

The data that support the findings of this study, which include EC-based nutrient sensor measurements for 37 soil samples subjected to 13 moisture treatments, are openly available in [GitHub Repository] at https://github.com/Melissateng97/Thesis_data/

REFERENCES

Ahmed, A. A., Leinweber, P., & Kühn, O. (2023). Advances in understanding the phosphate binding in soil: A computational chemistry perspective. *Science of The Total Environment*, *887*, Article 163692. https://doi.org/10.26434/chemrxiv-2022-lq2j3

Azam, H. M., Alam, S. T., Hasan, M., Yameogo, D. D. S., Kannan, A. D., Rahman, A., & Kwon, M. J. (2019). Phosphorous in the environment: Characteristics with distribution and effects, removal mechanisms,

treatment technologies, and factors affecting recovery as minerals in natural and engineered systems. *Environmental Science and Pollution Research*, *26*(20), 20183-20207. https://doi.org/10.1007/s11356-019-04732-y

Bauke, S. L., Amelung, W., Bol, R., Brandt, L., Brüggemann, N., Kandeler, E., Meyer, N., Or, D., Schnepf, A., Schloter, M., Schulz, S., Siebers, N., von Sperber, C., & Vereecken, H. (2022). Soil water status shapes nutrient cycling in agroecosystems from micrometer to landscape scales. *Journal of Plant Nutrition and Soil Science*, *185*(6), 773-792. https://doi.org/10.1002/jpln.202200357

Chadha, A., Florentine, S. K., Chauhan, B. S., Long, B., & Jayasundera, M. (2019). Influence of soil moisture regimes on growth, photosynthetic capacity, leaf biochemistry and reproductive capabilities of the invasive agronomic weed; *Lactuca serriola*. *PLOS ONE*, *14*(6), Article e0218191. https://doi.org/10.1371/journal.pone.0218191

Corwin, D. L., & Yemoto, K. (2020). Salinity: Electrical conductivity and total dissolved solids. *Soil Science Society of America Journal*, *84*(5), 1442-1461. https://doi.org/10.1002/saj2.20154

Costa, M. M., Queiroz, D. M. D., Pinto, F. D. A. D. C., Reis, E. F. D., & Santos, N. T. (2014). Moisture content effect in the relationship between apparent electrical conductivity and soil attributes. *Acta Scientiarum. Agronomy*, *36*(4), 395-401. https://doi.org/10.4025/actasciagron.v36i4.18342

Dimkpa, C., Bindraban, P., McLean, J. E., Gatere, L., Singh, U., & Hellums, D. (2017). Methods for rapid testing of plant and soil nutrients. In E. Lichtfouse (Ed.), *Sustainable agriculture reviews* (Vol. 25, pp. 1-43). Springer International Publishing. https://doi.org/10.1007/978-3-319-58679-3_1

Dion, P. (Ed.). (2010). *Soil biology and agriculture in the tropics* (Vol. 21). Springer Berlin Heidelberg. https://doi.org/10.1007/978-3-642-05076-3

Gavlak, R., Horneck, D., & Miller, R. O. (2005). *Soil, plant and water reference methods for the western region* (3rd ed.). Western Coordinating Committee.

Gee, G. W., & Bauder, J. W. (1986). Particle-size analysis. In A. Klute (Ed.), *Methods of soil analysis, part 1. Physical and mineralogical methods* (pp. 383-411). Soil Science Society of America, American Society of Agronomy. https://doi.org/10.2136/sssabookser5.1.2ed.c15

Gupta, H. V., Kling, H., Yilmaz, K. K., & Martinez, G. F. (2009). Decomposition of the mean squared error and NSE performance criteria: Implications for improving hydrological modelling. *Journal of Hydrology*, *377*(1-2), 80-91. https://doi.org/10.1016/j.jhydrol.2009.08.003

Heiniger, R., McBride, R., & Clay, D. (2003). Using soil electrical conductivity to improve nutrient management. *Agronomy Journal*, *95*(3), 508-519. https://doi.org/10.2134/agronj2003.0508

Herndon, E., Kinsman-Costello, L., Domenico, N. D., Duroe, K., Barczok, M., Smith, C., & Wullschleger, S. D. (2020). Iron and iron-bound phosphate accumulate in surface soils of ice-wedge polygons in arctic tundra. *Environmental Science: Processes & Impacts*, *22*(7), 1475-1490. https://doi.org/10.1039/D0EM00142B

Hossain, Md. D., Kashem, M. A., & Mustary, S. (2023). IoT based smart soil fertiliser monitoring and ML based crop recommendation system. *2023 International Conference on Electrical, Computer and Communication Engineering (ECCE)*, 1-6. https://doi.org/10.1109/ECCE57851.2023.10100744

Islam, M. R., Oliullah, K., Kabir, M. M., Alom, M., & Mridha, M. F. (2023). Machine learning enabled IoT system for soil nutrients monitoring and crop recommendation. *Journal of Agriculture and Food Research*, *14*, Article 100880. https://doi.org/10.1016/j.jafr.2023.100880

Klute, A. (1986). Water Retention: Laboratory Methods. In A. Klute (Ed.), *Methods of soil analysis, part 1. Physical and mineralogical methods* (pp. 635-662). Soil Science Society of America, American Society of Agronomy. https://doi.org/10.2136/sssabookser5.1.2ed.c26

Mazur, P., Gozdowski, D., & Wnuk, A. (2022). Relationships between soil electrical conductivity and sentinel-2-derived NDVI with pH and content of selected nutrients. *Agronomy*, *12*(2), Article 354. https://doi.org/10.3390/agronomy12020354

Miyamoto, T., Kameyama, K., & Iwata, Y. (2015). Monitoring electrical conductivity and nitrate concentrations in an Andisol field using time domain reflectometry. *Japan Agricultural Research Quarterly: JARQ*, *49*(3), 261-267. https://doi.org/10.6090/jarq.49.261

Nadporozhskaya, M., Kovsh, N., Paolesse, R., & Lvova, L. (2022). Recent advances in chemical sensors for soil analysis: A review. *Chemosensors*, *10*(1), Article 35. https://doi.org/10.3390/chemosensors10010035

Nottingham, A. T., Gloor, E., Bååth, E., & Meir, P. (2022). Soil carbon and microbes in the warming tropics. *Functional Ecology*, *36*(6), 1338-1354. https://doi.org/10.1111/1365-2435.14050

Nyakuri, J. P., Bizimana, J., Bigirabagabo, A., Kalisa, J. B., Gafirita, J., Munyaneza, M. A., & Nzemerimana, J. P. (2022). IoT and AI based smart soil quality assessment for data-driven irrigation and fertilisation. *American Journal of Computing and Engineering*, *5*(2), 1-14. https://doi.org/10.47672/ajce.1232

Obalum, S. E., Watanabe, Y., Igwe, C. A., Obi, M. E., & Wakatsuki, T. (2013). Improving on the prediction of cation exchange capacity for highly weathered and structurally contrasting tropical soils from their fine-earth fractions. *Communications in Soil Science and Plant Analysis*, *44*(12), 1831-1848. https://doi.org/10.1080/00103624.2013.790401

Omonode, R., & Vyn, T. (2006). Spatial dependence and relationships of electrical conductivity to soil organic matter, phosphorus, and potassium. *Soil Science, 171*(3), 223-238. https://doi.org/10.1097/01.ss.0000199698.94203.a4

Othaman, N. N. C., Isa, M. N., & Hussin, R. (2021). IoT based soil nutrient sensing system for agriculture application. *International Journal of Nanoelectronics and Materials*, *14*, 279-288.

Pansu, M., Gautheyrou, J., Pansu, M., & Pansu, M. (2006). *Handbook of soil analysis: Mineralogical, organic and inorganic methods*. Springer. https://doi.org/10.1007/978-3-540-31211-6

Reddy, Mr. Ch. S., Dasari, A., Meghna, G., Lekhna, S., & Shriya, S. (2023). Soil fertility analysis using IoT. *International Journal for Research in Applied Science and Engineering Technology*, *11*(6), 3738-3743. https://doi.org/10.22214/ijraset.2023.54183

Reeuwijk, L. P. van. (2002). *Procedures for soil analysis* (6th ed.). International Soil Reference and Information Centre.

Rhoades, J. D., Manteghi, N. A., Shouse, P. J., & Alves, W. J. (1989). Soil electrical conductivity and soil salinity: New formulations and calibrations. *Soil Science Society of America Journal*, *53*(2), 433-439. https://doi.org/10.2136/sssaj1989.03615995005300020020x

Rout, P. P., & Arulmozhiselvan, K. (2019). Effect of soil texture on drying pattern of soil moisture after saturation. *International Journal of Current Microbiology and Applied Sciences*, *8*(3), 697-704. https://doi.org/10.20546/ijcmas.2019.803.086

Sahu, G., Das, S., & Mohanty, S. (2020). Nutrient budgeting of primary nutrients and their use efficiency in India. *International Research Journal of Pure and Applied Chemistry*, 21*(11)*, 92-114. https://doi.org/10.9734/irjpac/2020/v21i1130227

Schulten, H.-R., & Schnitzer, M. (1997). The chemistry of soil organic nitrogen: A review. *Biology and Fertility of Soils*, *26*(1), 1-15. https://doi.org/10.1007/s003740050335

Seyedmohammadi, J., Navidi, M. N., & Esmaeelnejad, L. (2019). Geospatial modeling of surface soil texture of agricultural land using fuzzy logic, geostatistics and GIS techniques. *Communications in Soil Science and Plant Analysis*, *50*(12), 1452-1464. https://doi.org/10.1080/00103624.2019.1626870

Tamad, T., Ismangil, I., & Maryanto, J. (2020). The biochemical characteristics of phosphate bacteria capable of increasing soil phosphorus bioavailability in Andisols. *Soil Science Annual*, *71*(2)*,* 125-132. https://doi.org/10.37501/soilsa/122403

Thiemig, V., Rojas, R., Zambrano-Bigiarini, M., & De Roo, A. (2013). Hydrological evaluation of satellite-based rainfall estimates over the Volta and Baro-Akobo Basin. *Journal of Hydrology*, *499*, 324-338. https://doi.org/10.1016/j.jhydrol.2013.07.012

Yu, A. J., Lin, X., Zhu, J., He, H., & Li, L. (2023). Environmental effects on ammonium adsorption onto clay minerals: Experimental constraints and applications. *Applied Clay Science*, *246*, Article 107165. https://doi.org/10.1016/j.clay.2023.107165

Zhao, X., Wang, J., Zhao, D., Sefton, M., & Triantafilis, J. (2022). Mapping cation exchange capacity (CEC) across sugarcane fields with different comparisons by using DUALEM data. *Journal of Environmental and Engineering Geophysics*, *27*(4), 191-205. https://doi.org/10.32389/JEEG22-002

Žinete, J. (2023). The role of NPK fertilisers in modern agriculture: Fuelling crop growth and maximising yields. *Internation Journal of Manure and Fertiliser*, *11*(2).